Comparison of powdered and colloidal SiO_2 nanofillers in nanocomposite pervaporation desalination membranes

Indah Prihatiningtyas D.S[1, 2, a)], Maria Sandra Reyes Ballesteros[1, b)], Tamrin[2, c)], and Bart Van der Bruggen[1, 3, d)]

Author Affiliations
[1]*Department of Chemical Engineering, KU Leuven, Celestijnenlaan 200F, box 2424, B-3001, Leuven, Belgium.*
[2]*Department of Chemical Engineering, Mulawarman University, Jalan Sambaliung No.9, Sempaja Selatan, Samarinda, Kalimantan Timur, Indonesia.*
[3]*Faculty of Engineering and the Built Environment, Tshwane University of Technology, Private Bag X680, Pretoria 0001, South Africa.*

Author Emails
[a)] Corresponding author: indah.unmul@gmail.com
[b)] maria.srb@gmail.com
[c)] fts_tamrin@ft.unmul.ac.id
[d)] vander.brugen@gmail.com

Abstract. In this work, cellulose triacetate/SiO_2 nanocomposite pervaporation (PV) membranes were successfully fabricated in order to enhance the membrane performance for desalination. Two sources of SiO_2 nanoparticles; powdered SiO_2 and the colloidal silica solution (LUDOX AS40) were investigated. The fabricated PV nanocomposite membranes were characterized to study the membrane morphology by Scanning electron microscopy (SEM), the chemical composition by Fourier transform infrared (FTIR), and the surface hydrophilicity by water contact angle. SiO_2 colloidal nanoparticles disperse more better compared to the SiO_2 powder in the dope solution. Therefore, the SiO_2-colloidal nanoparticles were even distributed on the membrane surface. Furthermore, membrane performance was investigated to treat the feed solution at 30 g L^{-1} of sodium chloride (NaCl) at operating temperature of 70 ^oC. Pervaporation (PV) experiments showed that incorporating 1% SiO_2-powder nanoparticles into a CTA membrane improved the water flux by 123% compared to pristine CTA (from 2.16 kg m^{-2} h^{-1} to 4.82 kg m^{-2} h^{-1}), while added 1% SO_2-collodial nanoparticles increased the water flux by 257% (from 2.16 kg m^{-2} h^{-1} to 7.72 kg m^{-2} h^{-1}), both of CTA/SiO_2 nanocomposite membranes kept the salt rejection above 99 %. Additionally, the CTA/SiO_2 colloidal nanocomposite membrane has a positive stability of PV desalination performance for 12 hours separation. Hence, the results suggests that the developed CTA/SiO_2-colloidal nanocomposite PV membrane is the best for desalination.

INTRODUCTION

Water pollution, and groundwater exploitation result in a decreasing quality of available natural water resources, while the world population increases along with growing living standards leading to a higher water consumption; hence these conditions lead to water scarcity. Desalination is becoming an emerging technology to provide a potable water to overcome water scarcity, because there is an abundance of water resources in the world of which almost 97% is seawater [1]. Pervaporation (PV) is a membrane process with growing interest as a potential alternative for desalination due to its high salt selectivity; there is no need for extensive pre-treatment for the feed solution, and membranes for desalination are hydrophilic, yielding less fouling propensity. In addition, pervaporation is able to handle feed streams with high salt concentrations [2]. Polymers are widely used as membrane material. Polymers have

advantages such as a low cost, mechanical stability, high flux, and simple fabrication; however, their disadvantages are a low selectivity and chemical stability. There is a trade-off between permeability and selectivity in the membrane performance and the main challenge of PV for desalination is the low water flux due to dense membrane properties [3],[4].

Several studies have developed nanocomposite membranes by incorporating inorganic or organic nanoparticles (NPs) into a polymeric film, to increase the performance and to enhance the membrane lifetime [5]. Common inorganic and organic materials have been used for fabricating nanocomposite membranes, such as TiO_2 [6], SiO_2 [7],[8], Al_2O_3 [9], graphene oxide (GO) [10], carbon nanotubes [11], and cellulose nanocrystals [3].

In this study, nanocomposite PV membranes consisting of cellulose triacetate (CTA) incorporated with SiO_2 nanoparticles were prepared by solution casting. CTA is a cellulose based material that is attractive for desalination application because it has a great potential for salt rejection, an adequate mechanical strength, a fairly low cost, a better oxidant resistance, a lower fouling tendency and can be produced as a dense film [12]. While silica (SiO_2) nanoparticles show a low toxicity, their surface is hydrophilic and easy to modify with functional chemical groups. Besides, SiO_2 nanoparticles have been integrated with polymeric membranes and applied for water and wastewater treatment due to their advantages such as: show excellent selectivity and chemical stability, have good mechanical and thermal resistance, high hydrophilicity, and fouling resistance [13]-[16]. Silica nanoparticles also have an excellent biocompatibility and mechanical stability for thin film nanocomposite (TFN) membranes fabrication [17]. The pervaporation nanocomposite CTA/SiO_2 membranes with two sources of SiO_2 nanoparticles i.e powder and colloidal were prepared and characterized. Furthermore, the membrane performance in terms of water flux and salt rejection were investigated and compared.

EKSPERIMENTAL

Chemicals and Materials

Cellulose triacetate (CTA, acetyl content 43-44 %, molecular weight 966.845 g/mol) was obtained from ACROS, dimethyl sulfoxide (DMSO, 99.5 %, reagent) was purchased from Fisher Chemical. Two sources of SiO_2 nanoparticles were employed in this project : Colloidal silica, LUDOX AS-40 (40 wt.% suspension in water) from Sigma Aldrich with particle sizes of 20-24nm and SiO_2 powder from Aladdin (product no: S104600) with particle sizes of 7-40nm respectively. Sodium chloride (99.5% purify) was purchased from Acros Organics and was employed as the solute in the feed solution during pervaporation. All chemicals were used without further purification.

Membrane Preparation

Membranes were prepared by the solution casting method followed by the solvent evaporation. The SiO_2 suspensions were prepared by dispersing 1 wt.% SiO_2 (with respect to the dope solution weight) in DMSO for 3 hours using a magnetic stirrer at a speed of 1000 rpm. Then, 6 wt.% cellulose triacetate (CTA) was loaded into the SiO_2 suspensions, followed by stirring for 4 hours at 75 °C. Next, the dope solutions were placed in a sonicating water bath for 2 hours, then left stirring for overnight. Next, the dope solutions were left for 4 hours at room temperature then cast on the glass plate with an automatic casting device. The casting blade height of 200 µm was used at room temperature and at the lowest speed setting (0.98 cm s^{-1}) with a relative humidity between 34 and 44 %. The cast films were dried in a vacuum oven for 4 hours at 60 °C and pressure of 0.169 bar.

Characterization of the membrane

Fourier transform infrared (FTIR)

The functional groups on the membrane surfaces were analyzed by Fourier transform infrared spectroscopy (FTIR, Perkin Elmer spectrum 100 with universal ATR sampling accessory, USA). The transmittance spectra were directed from 650 to 4000 cm^{-1} at room temperature and at least 4 scanning for each sample were conducted.

Scanning electron microscopy (SEM)

The surface and the cross-section morphologies of the composite membranes were visualized by SEM imaging via XL30 FEG field-emission scanning electron microscope (FE-SEM, Netherlands). The samples were sputter-coated with a 1.5 – 2 nm gold layer. A voltage of 10 kV was selected to obtain the surface and the cross-section images

Water contact angle (WCA)

Water contact angle measurements were conducted to study the hydrophilicity of the membranes. A standard contact angle apparatus (Krüss GmbH Germany, model: DSA 10-Mk2) was operated at room temperature and the measurements were performed using a drop-shape analysis software. The MilliQ water volume was set at 2 µl at a rate of 24.79 µl min^{-1} then the MiliQ water (2 µL) was dropped onto the membrane surface for each measurement. Five randomly selected locations on each sample were recorded then reported as the contact angle measurement.

Water uptake (WU)

Water uptake of the membranes was measured by cutting the membrane in pieces of 2 cm × 2 cm. The specimens were immersed in MiliQ water at room temperature for 24 hours. After 24 hours, the surface of wet specimens was dried using an absorbent paper, then the mass was recorded (W_w). The specimens were dried in an oven at 105 ºC for 24 hours, then the dry specimens were weighed (W_d). The water uptake (WU) was calculated as follows :

$$WU = \frac{W_w - W_d}{W_d} \, x \, 100\% \quad (1)$$

Membrane performance: water flux and rejection

A pervaporation study using the fabricated membranes was conducted using a customized setup, schematically shown in Figure 1.

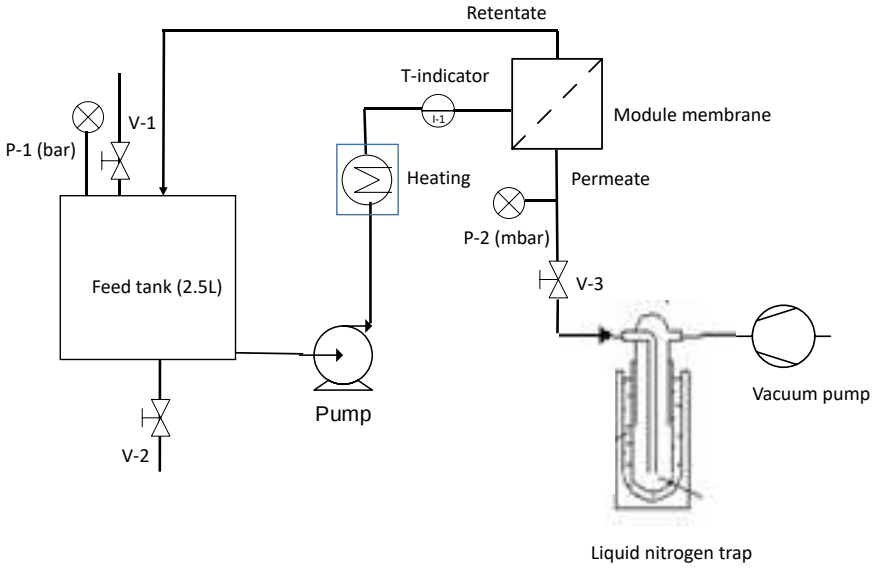

FIGURE 1. Schematic flow chart of the experimental setup for pervaporation desalination.

Pervaporation works simply by applying vacuum (Edwards two stage model E2M2, vacuum pressure 0.1 mbar - 1 mbar) at the downstream. The vacuum pump was employed to create a vapor pressure difference across the membranes. A feed solution of 30 g L^{-1} NaCl in MiliQ water was filled in a 2.5 L stainless steel tank. Pervaporation was operated at 70 °C at a feed flow rate of 70 - 80 L h^{-1}. The self-made flat sheet membrane with an effective membrane surface area of 19.63 cm^2 (diameter = 5 cm) being mounted onto the membrane cell unit. The pervaporation

experiment was two hours and the permeate samples were collected at determined time interval. The water flux J_w (kg m^{-2} h^{-1}) was calculated as below equation: [1]

$$J_w = \frac{m}{A.t} \quad (2)$$

The salt rejections R (%) were determined from the following equation:

$$Rejection\ (\%) = \frac{C_f - C_p}{C_f}\ x\ 100\% \quad (3)$$

Where m is the permeate weight collected (kg), A is the effective membrane area (m^2), t is the time period required to collect a certain amount of permeate (h), C_f and C_p are the salinity in the feed and permeate solutions, respectively. The salinity value was measured by a conductivity meter model Consort-C831.

RESULT AND DISCUSSION

Figure 2 shows the dope solutions for preparing membrane in different types of SiO_2 nanoparticles. The picture shows that the dope solution prepared with SiO_2 powder is less transparent appearance than the SiO_2 colloidal solution. This indicates that SiO_2 colloidal nanoparticles disperses more preferentially compared to the SiO_2 powder nanoparticles.

(a) (b)

FIGURE 2. The dope solution for fabricating membrane : (a) SiO_2 powder nanoparticles and (b) SiO_2 colloidal nanoparticles.

Fourier transform infrared (FTIR)

FTIR spectrum of pristine CTA membrane, CTA/SiO_2-powder membrane and CTA/SiO_2-colloidal membrane are showed in Figure 3. The characteristic band of typical cellulose triacetate at 1739 (C=O), 1370 (-CH_3), 1210 and 1032 (C-O-C) are presented in the FTIR spectra of the CTA/SiO_2-powder and CTA/SiO_2-colloidal membranes [18]. Compared with the spectrum of the pristine CTA membrane, new peaks at 801 that represents to Si-O-Si band was observed for CTA/SiO_2-powder and CTA/SiO_2-colloidal membranes [19]. This peak confirms that SiO_2 nanoparticles are present in the CTA membrane. Figure 3 also shows that intensity at peak 801 for CTA/SiO_2-collodial membrane is lower than CTA/SiO_2-powder membrane which reveals that the concentration of SiO_2 nanoparticles in the membrane is higher [20].

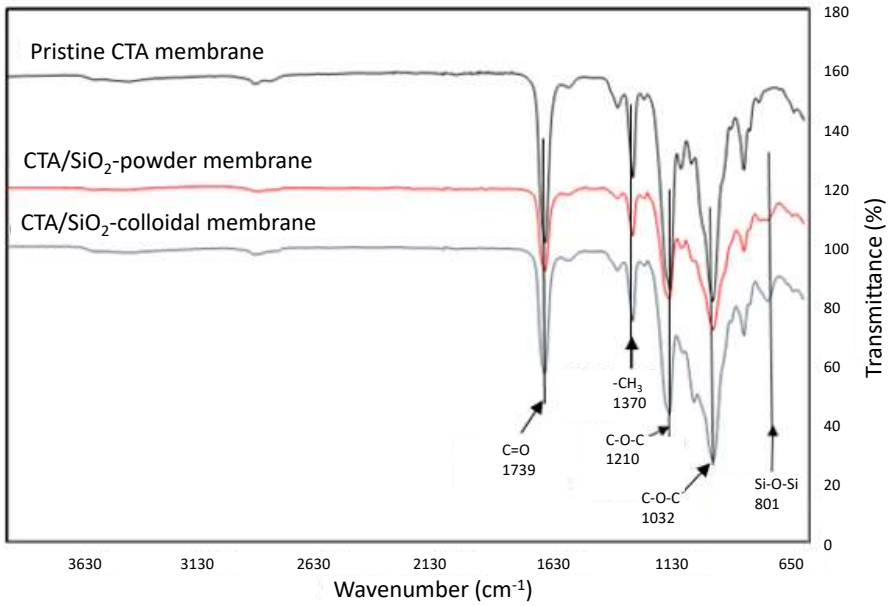

FIGURE 3. FTIR spectrum of pristine CTA membrane, CTA/SiO_2-powder membrane and CTA/SiO_2-colloidal membrane.

Scanning electron microscopy (SEM)

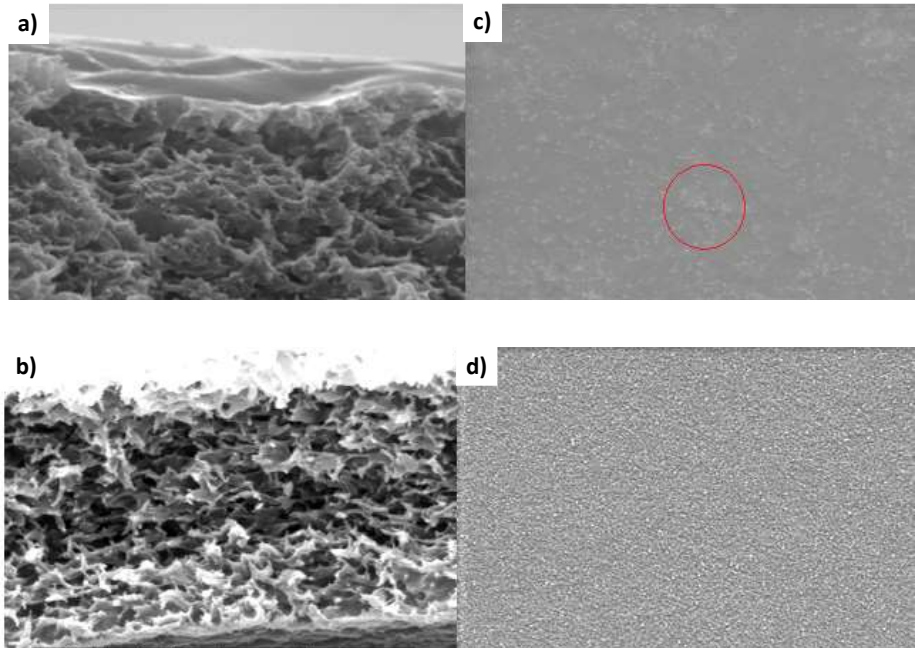

FIGURE 4. SEM images of cross section (a) CTA/SiO_2-powder membrane and b) CTA/SiO_2-colloidal membrane, the membrane surface of (c) CTA/SiO_2-powder membrane and d) CTA/SiO_2-colloidal membrane (magnification 10000).

Photographed images of the pristine CTA membrane and modified CTA membranes are shown in Figure 4. The incorporation of SiO_2 nanoparticles in the CTA membrane showed as a white spot on the membrane surface (see Figure 4a and 4b). As shown in Figure 4b, the CTA/SiO_2-colloidal membrane has a more homogeneous distribution compared to the CTA/SiO_2-powder membrane (see Figure 4a). It indicates that the SiO_2 colloidal nanoparticles have a better distribution within the polymeric matrix and less aggregation compared to the SiO_2 powder nanoparticles.

Red circle as shown in Figure 4c presents the aggregation of SiO_2 powder nanoparticles. The cross-section of the membranes as presented in Figure 4a and 4b describes that both the membrane have a similar morphology, i.e a sponge-like structure with dense top and bottom layers.

Water contact angle (WCA) and water uptake (WU)

Figure 5a illustrates the water contact angle values of pristine CTA membrane, CTA/SiO_2-powder and SiO_2-colloidal membranes. The water contact angle values as depicted in Figure 5a clarifies that all prepared membranes are hydrophilic. The initial contact angle decreases from 68.9º to around 62º and 63º for CTA membrane modified by SiO_2 nanoparticles. The modified CTA membrane by incorporating SiO_2 nanoparticles shows a slight decrease of water contact angle, however, the water uptake increases from the pristine CTA membrane as shown in Figure 5b. The water uptake enhancement is due to the presence of hydrophilic nanoparticles in the membrane surface which is strengthening its water affinity [21],[22]. Figure 5b describes that CTA/SiO_2-colloidal membrane shows the higher of water uptake than CTA/SiO_2-powder membrane due to the uniform of silica nanoparticles on the membrane as shown in Figure 4d.

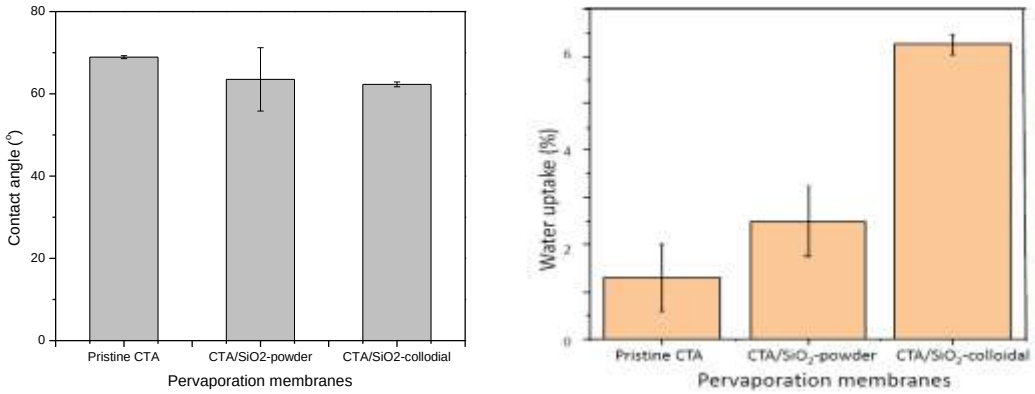

FIGURE 5. Contact angle (a) and water uptake (b) of fabricated pervaporation membranes.

Pervaporation membrane performance

Figure 6 manifests the average of the water flux and NaCl rejection of each pristine CTA and CTA/SiO_2 nanoparticles membrane. The water flux increases from 2.16 kg m^{-2} h^{-1} to 4.82 and 7.72 kg m^{-2} h^{-1} when SiO_2 nanoparticles added in the pristine CTA membrane, while the NaCl rejection is still retained above 99%. This increment is due to the addition of SiO_2 nanoparticles into the CTA membranes increases the hydrophilicity as described in the increasing of water uptake (see Figure 5b) which is more water molecules absorbed into the membrane. Addition, incorporating SiO_2 nanoparticles into CTA membrane could offer extra permeation pathways which also donate to the higher water flux. Figure 6 reveals that integrating SiO_2 colloidal nanoparticles has the highest water flux compared to the other fabricated membranes. NaCl retention could be kept above 99% due to the dense structure on the surface of pervaporation membrane which performs as a selective layer [23], also because the non-volatility and low diffusivity of NaCl . The membrane performance of CTA/SiO_2-colloidal membrane for 12 hours was observed. Figure 7 describes that the water flux is approximately constant and the NaCl rejection is still kept above 99%.

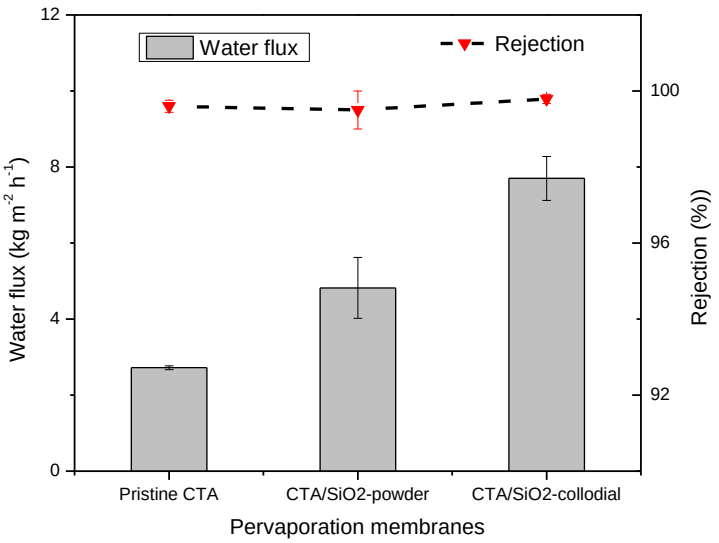

FIGURE 6. Pervaporation desalination performance of fabricated pervaporation membranes (At feed temperature of 70 ^{o}C and feed solution of 30 g L^{-1} NaCl).

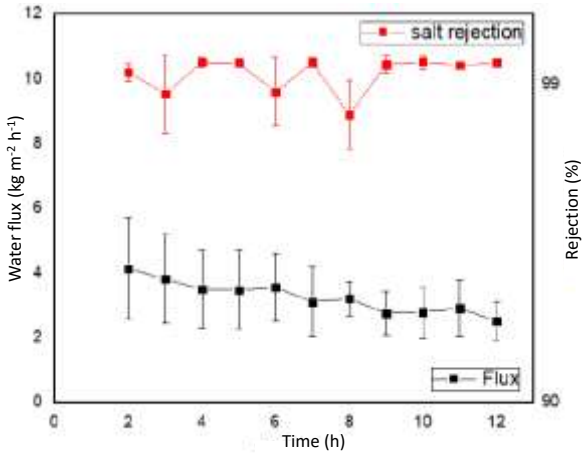

FIGURE 7. Pervaporation desalination performance of CTA/SiO_2-colloidal membrane for 12 hours (At feed temperature of 70 ^{o}C and feed solution of 30 g L^{-1} NaCl).

CONCLUSION

Cellulose triacetate/SiO_2 nanocomposite pervaporation (PV) membranes were successfully fabricated with two sources of SiO_2 nanoparticles, i.e SiO_2 powder and SiO_2 colloidal. Integrating SiO_2 nanoparticles in the CTA membrane enhanced the water flux of the membrane. The dope solution of CTA/SiO_2-powder was less transparent appearance which showed that SiO_2 colloidal nanoparticles dispersed more better compared to the SiO_2 powder nanoparticles. Hence, the SiO_2-colloidal nanoparticles were uniform distributed on the membrane surface. Furthermore, the water flux of SiO_2-colloidal membrane was higher compared to SiO_2-powder membrane, which enhanced by 257% from the pristine CTA membrane (from 2.16 to 7.72 kg m^{-2} h^{-1}). All fabricated pervaporation membranes showed a high selectivity by maintaining the NaCl rejection above 99%. Moreover, the CTA/SiO_2 colloidal nanocomposite membrane had a positive stability of PV desalination performance for 12 hours separation.

ACKNOWLEDGMENTS

This research was supported by the Indonesia Endowment Fund for Education (LPDP). The authors would like to thank to Christine Wouters (KU Leuven) for measuring FTIR.

REFERENCES

[1] E. Hameeteman, "Future Water (In) security : Facts , Figures , and Predictions Future Water (In) Security : Facts , Figures , and Predictions," Glob. Water Inst. (2013), p. 16
[2] Q. Wang, N. Li, B. Bolto, M. Hoang, and Z. Xie: Desalination Vol. 387 (2016), pp. 46–60
[3] I. Prihatiningtyas, A. Volodin and B. Van der Bruggen: Ind. Eng. Chem. Res. Vol.58, no. 31 (2019), pp. 14340–14349
[4] X. Cheng, F. Pan, M. Wang, W. Li, Y. Song, G. Liu, H. Yang, B. Gao, H. Wu, Z. Jiang: J. Memb. Sci., Vol. 541, no. July (2017) , pp. 329–346
[5] J. H. Jhaveri and Z. V. P. Murthy: Vol. 57, no. 55. Elsevier Inc., (2016).
[6] B. Khorshidi, I. Biswas, T. Ghosh, T. Thundat and M. Sadrzadeh: Sci. Rep., Vol. 8, no. 1 (2018), pp. 1–10
[7] M. Zargar, Y. Hartanto, B. Jin and S. Dai: J. Memb. Sci., vol. 519 (2016), pp. 1–10
[8] M. Zargar, Y. Hartanto, B. Jin and S. Dai: J. Memb. Sci., vol. 541, no. June (2017), pp. 19–28
[9] Y. Song, D.K. Wang, G. Birkett, W. Martens, M.C. Duke, S. Smart, J.C. Diniz Da Costa: Sci. Rep. Vol. 6, no. July (2016), pp. 1–10
[10] K. Xu, B. Feng, C. Zhou, and A. Huang: Chem. Eng. Sci. Vol. 146 (2016), pp. 159–165
[11] G. Yang, Z. Xie, M. Cran, D. Ng and S. Gray: J. Memb. Sci. Vol. 579, no. January (2019), pp. 40–51
[12] X. Chen, J. Xu, J. Lu, B. Shan and C. Gao: Desalination Vol. 405 (2017), pp. 68–75
[13] L.Y. Ng, L.Y, A.W. Mohammad, C.P. Leo, N. Hilal: Desalination Vol. 308 (2013), pp. 15–33
[14] N. Torasso, A. Vergara-Rubio, P. Rivas-Rojas, C. Huck-Iriart, A. Larrañaga, A. Fernández-Cirelli: J. Environ. Chem. Eng. Vol. 9 (2021) 104664
[15] J. Yin, E.S. Kim, J. Yang, B. Deng: J. Membr. Sci. Vol. 423-424 (2012), pp. 238–246
[16] N. Rosdi, M.N.M. Sokri, N.M. Rashid, M.S. Che Chik, M.S. Musa: J. Appl. Membr. Sci. Technol. Vol. 23 (2019), pp. 63–72
[17] M. Zargar, Y. Hartanto, B. Jin and S. Dai: J. Memb. Sci. Vol. 521 (2017), pp. 53–64
[18] M. Amara, O. Arous, F. Smail, H. Kerdjoudj, M. Trari, and A. Bouguelia : Journal of hazardous materials, 169(1-3) (2009), pp. 195–202
[19] P. J. Launer. Infrared analysis of organosilicon compounds: spectra-structure correlations. Silicone compounds register and review (1987), pp. 100
[20] I. Prihatiningtyas, G. A. Gebreslase, and B. Van der Bruggen: Desalination Vol. 474 (2020), pp. 114198,
[21] M. R. Esfahani et al., Sep. Purif. Technol. Vol. 213 (2019), pp. 465–499
[22] N. Sobel et al., Beilstein J. Nanotechnol. Vol. 6, no. 1 (2015), pp. 472–479
[23] I. Prihatiningtyas, Y. Hartanto, and B. Van der Bruggen: Chem. Eng. Sci., (2020), pp. 116276